



Removal of Humic Acid from Water by Adsorption Using Chitosan and Metal Organic Framework ZIF 8 Loaded Chitosan Adsorbents

Nilufer Hilmioglu · Esra Yumat

Received: 19 December 2023 / Accepted: 14 March 2024
© The Author(s) 2024

Abstract Water is the most necessary need for life on the earth. There are a lot of organic pollutants in water. One of the organic pollutants is natural organic substances. Humic acid, a natural organic substance, turns into very harmful substances along with other pollutants. In this study, the humic acid removal from aqueous solution by adsorption using chitosan and chitosan/ZIF 8 composite spheres was examined. Chitosan spheres cross-linked with epichlorohydrin (ECH) and composite spheres consisting of metal organic framework ZIF8 and chitosan were prepared as adsorbents. Equilibrium, kinetic, and thermodynamic studies were investigated for humic acid adsorption by pristine chitosan-ECH and composite chitosan/ZIF 8 adsorbents. Chemical adsorption was found to be compatible with the Freundlich isotherm model and the pseudo-first-order kinetic model for pure chitosan adsorbents. Studies were carried out using chitosan/ZIF8 composite adsorbent, and the most suitable models for chemical adsorption were determined as Langmuir isotherm and pseudo-second order kinetic model. The response surface method was applied with the design expert program to determine the optimum experimental conditions. The adsorption tests were carried out using chitosan-ECH, ZIF 8 and chitosan/ZIF 8 adsorbents for specified

optimum conditions, and the humic acid removal was determined as 95.1%, 98.3%, and 97.3%, respectively. In addition, desorption was performed using chitosan-ECH and chitosan/ZIF 8 spheres, and the desorption efficiency was found to be 20.9% and 82.5%, respectively. It has been observed that the developed adsorbents have potential in removing humic acid from water.

Keywords Adsorption · Humic Acid · Chitosan/ ZIF 8

1 Introduction

Water is the most important substance for living life (Gundag, 2017). There are organic and non-organic pollutants that are unwanted in the water. Natural organic substances are the organic pollutants (Lorenc et al., 2005). The contents of natural organic substances are humic acid, fulvic acid, humin, amino acids, etc. Natural organic substances have aliphatic, aromatic, carboxylic (-COOH), and phenolic groups (Gundag, 2017). Generally, groundwater and surface waters may have 20–30 mg/L humic substances (Wang et al., 2012). Humic acid constitutes a significant part of humic substances. Humic acid itself is not harmful. When humic acid mixes with water, it binds substances such as pesticides and heavy metals and increases their transport. During water disinfection, humic acid reacts with chlorine to form

N. Hilmioglu (✉) · E. Yumat
Department of Chemical Engineering, Kocaeli University,
41001 Kocaeli, Turkey
e-mail: niluferh@kocaeli.edu.tr

trihalomethane that is carcinogenic (Dehghani et al., 2016).

Humic acid can cause changes of the color, smell, and taste of water. Moreover, this situation reduces the efficiency of water treatment plants (Khan et al., 2015). High amounts of humic acid intake causes etiological diseases (Lorenc-Grabowska & Gryglewicz, 2005). For all these reasons, humic acid removal from water is an important research topic. There are the methods that are coagulation, adsorption, ion exchange, and membrane process for removing humic acid from water (Soylu, 2011). Adsorption appears to be an effective technique for reasons such as easy and simple of design (Dehghani et al., 2017). Different adsorbents such as chitin, chitosan, bentonite, activated carbon, graphite, clay minerals (montmorillonite), kaolin, and zeolite can be used in the adsorption process (Hartono et al., 2009). Humic acid removal value is low with the conventional adsorbents (Wan Ngah and Musa, 1998). For increasing the performance of the adsorption, it is a requirement to develop an alternative adsorbent that can show high and versatile affinity for humic acid.

In the study conducted by Dehghani et al. (2018), bentonite-chitosan adsorbent was prepared for humic acid removal from water, and its capacity was 91.4 mg/g. In the another test by Yan et al. (2005), humic acid adsorption was carried out from aqueous solutions using chitosan hydrogel spheres, and its capacity was calculated as 0.7 mg/g. In the study managed by Zhang et al. (2003), chitosan dipped of polyethylene terephthalate and examined for humic acid removal and the maximum capacity was stated 0.407 mg/g. In the study that is humic acid adsorption from water using chitin and chitosan, the amount of adsorption capacity was 28.88 mg/g (Wan Ngah et al., 1998). In a study by Soleimani et al. (2019), they examined removing of humic acid from water by pumice stones modified with five different acids, and it was found maximum to be 65.75 mg/g using sulfuric acid modified pumice adsorbent. In the study controlled by Bougdah et al. (2019), the highest adsorption value by chitosan adsorbent was determined as 65.35 mg/g. In the study of Jampa et al. (2020), the humic acid adsorption was examined by nano ZIF 8 adsorbent, and the maximum capacity was determined as 42.9 mg/g. In a study directed by Wan Ngah et al. (2008), they focused on the removal by chitosan spheres cross-linked with epichlorohydrin

(ECH), and the adsorption capacity maximum value was 44.84 mg/g. In the experimental study controlled by Lin and Chang (2015), the adsorption of humic acid from water was investigated by ZIF 8 adsorbent, and the highest capacity was 11.7 mg/g. Lin et al. (2012) studied on the adsorption of humic acid from water by chitosan/zeolite composites; it was found to be 164 mg/g.

Chitosan is a more economical and natural biopolymer (Mathur et al., 1990). Chitosan, a cationic biopolymer, is formed by chitin deacetylation. Chitosan is a biocompatible polymer and a very good adsorbent due to its hydrophilic properties (Dehghani et al., 2018). In our previous studies, chitosan was used to separate harmful substances from water by adsorption (Oktor and Hilmioglu, 2021, Oktor et al., 2023).

Zeolitic imidazolate frameworks (ZIFs) are a subclass of metal-organic structure. ZIFs that are crystalline porous materials have high surface area (Lin & Zhan, 2012) and better in terms of chemical and thermal stability. ZIF 8 is made by bonding zinc or cobalt to metal imidazole groups (Park et al., 2016). ZIF 8 has high chemical stability in aqueous solution and large pore structure (Park et al., 2006).

In this study, pristine and composite adsorbent were prepared by chitosan and chitosan loaded ZIF 8 respectively. Humic acid removal by this composite adsorbent has not been studied before in the literature. It is aimed to produce these adsorbents. Firstly, pristine chitosan adsorbent spheres were produced with chitosan solution, whose mechanical properties were increased by using epichlorohydrin (ECH) cross-linking agent. Humic acid removal efficiency from water was examined with the chitosan sphere adsorbents. Then, 10% ZIF 8 suspension was added to the chitosan solution obtained without cross-linking agent, and a new composite adsorbent was obtained. Humic acid removal efficiency from water was examined with the composite adsorbent. Design expert 12 student version a statistical data analysis program, was used to determine the optimum adsorption experiment parameters. Optimum operating parameters were determined from the adsorption experiments performed using chitosan-ECH adsorbent sphere, and adsorption experiments were carried out in ZIF 8-doped chitosan composite adsorbent sphere with the same parameters. Moreover, the effects of humic acid solution concentration, adsorbent dosage, and temperature, which were

determined as variable parameters, on humic acid removal efficiency were examined. In addition, isotherm, kinetic, thermodynamic, and desorption tests made by two different adsorbents, and the effectiveness of the adsorbents was examined comparatively.

2 Materials and Method

2.1 Materials

Humic acid, chitosan, acetic acid, epichlorohydrin, sodium hydroxide, 2-methylimidazole, zinc nitrate hexahydrate, and methanol were purchased from Sigma-Aldrich.

2.2 Preparation of Pure Chitosan Adsorbents

The polymer solution was prepared by dissolving 2% by weight chitosan polymer with 2% by weight acetic acid. Homogeneous chitosan solution was cross-linked using epichlorohydrin (ECH) at 8% of the polymer weight. Adsorbent spheres were formed by dropping this solution into 2 M sodium hydroxide. The spheres were washed by water until the neutral pH and dried first at room temperature and then at 60 °C.

2.3 Preparation of ZIF 8 Loaded Chitosan Composite Adsorbents

The prepared solutions of methyl imidazole and zinc nitrate hexahydrate in methanol were mixed. The formed ZIF 8 crystals were taken from the solution by centrifugation and washed with methanol and then dried at 80 °C. It was subjected to heat treatment at 180 °C for activation (Venna et al., 2010). Ten percent (wt.) ZIF 8 suspension was added little by little into the 2% (wt.) chitosan solution. Composite spheres were formed by dropping the homogeneous solution into NaOH solution. As with pristine spheres, composite spheres were also ready after washing with water and drying operations.

2.4 Adsorption Tests

Stock solution of humic acid was obtained by dissolving humic acid with water and a very small amount of NaOH. Synthetic humic acid solution at the desired

concentrations was prepared by the way of dilution of the stock solution. The maximum absorption wavelength of the prepared humic acid solutions was found to be 300 nm in the UV–vis spectrophotometer.

Studies on optimum pH and contact time were carried out with 0.5 g chitosan-ECH sphere amount and 55 mg/L humic acid concentration. Among the pH values studied, the best efficiency was determined as pH 4. The time to reach equilibrium was determined as 110 min.

Adsorption tests were carried out at different humic acid concentrations (10, 55, 100 mg/L), different adsorbent dosage (0.5, 1, 1.5 g), and different temperatures (25, 35, 45 °C).

The amount of adsorbed humic acid (mg/g) is calculated according to the mass balance in Eq. (1):

$$q_e = ((C_o - C_e)/m)XV \quad (1)$$

C_o and C_e are the humic acid concentrations before and after adsorption (mg L^{-1}), respectively; V is the volume of the humic acid solution (L); and m is the weight of the adsorbent (g) (Wan Ngah et al., 2008).

2.5 Desorption Tests

For the desorption study, pristine chitosan spheres were collected after the optimum adsorption study (1.5 g adsorbent dosage, 10 mg/L humic acid concentration, pH 4, and contact time 110 min) and dried at room temperature (25 °C) for 2 days. Then, the desorption efficiencies of the dried spheres were examined at 1 M HCl acid concentration with different contact times (60–90–120 min) (Wan Ngah et al., 2008).

The percentage of desorbed humic acid (HA) is calculated using Eq. (2) (Wan Ngah et al., 2008):

$$\%D = (C_{de}/C_{ae}) * 100 \quad (2)$$

C_{de} is HA concentration at desorption equilibrium (mg/L) and C_{ae} is HA concentration at adsorption equilibrium (mg/L).

2.6 Statistical design

The response surface method, one of the experimental design methods, is used to determine optimum parameters among multiple data within a process or processes. Variables that can be controlled within these

multiple data are called independent, and those that we cannot influence are called dependent variables (Rodrigues et al., 2009). With developing technology, the response surface method, which is a statistical data analysis program and more efficient than classical trial and error methods, is more preferred. With classical testing methods, experiments performed with only one variable change took too much time, and the amount of experiments was high. In experiments carried out using the response surface method, a less time-consuming and therefore less costly process occurs in which each variable parameter is used. It offers more systematic and comprehensive analysis compared to the experimental stages carried out with the classical method.

The effects of variable parameters entered into the system on the response are observed, and the optimum experimental parameters can be determined by the system (Hilmioglu, 2022).

Box-Behnken design model, one of the statistical data analysis methods, has a mathematical relationship between the response surface and the determined variables (Mohammed, 2014).

For the RSM program (Box-Behnken design model), three variables as adsorbent dosage (0.5; 1; 1.5 g), humic acid solution concentrations (10, 55, 100 mg/L), and temperature (25, 35, 45 °C) are used to determine the result. Humic acid removal (%) effect was investigated. In line with these optimum experimental data, experiments were carried out under optimum conditions with chitosan spheres prepared with 10% ZIF8 additive. Thus, the % humic acid removal efficiency of pristine chitosan and ZIF 8-doped chitosan composite spheres was compared under the same conditions.

2.7 Isotherm, Kinetic, and Thermodynamic Studies

2.7.1 Isotherm Models

The Langmuir model isotherm accepts that the adsorption process occurs as a single layer on a homogeneous surface. Langmuir model is as given in Eq. (3) (Tumkor, 2018):

$$1/q_e = 1/q_m + 1/(bq_m C_e) \quad (3)$$

The line is obtained by drawing the graph of $1/q_e$ against $1/C_e$, intercept is $1/bq_m$, and slope is $1/q_m$.

K_L is a dimensionless parameter. K_L is expressed in Eq. (4):

$$K_L = 1/(1 + bC_0) \quad (4)$$

q_e is amount of substance adsorbed per unit adsorbent (mg/g), C_e is amount of substance remaining in solution (mg/L), K_L is Langmuir isotherm constant, q_m is maximum adsorption capacity of the adsorbent (mg/g), b is constant, and C_0 is initial concentration of the solution (mg/L).

The Freundlich isotherm model states that the multilayer adsorption process occurs on the heterogeneous adsorbent surface because of the diversity of adsorptive sites (Sahbaz & Acikgoz, 2017).

Freundlich model is as given in Eq. (5) (Tumkor, 2018):

$$\log q_e = \log k_F + (1/n)\log C_e \quad (5)$$

The graph is plotted $\log q_e$ versus $\log C_e$, the slope is $1/n$, and its intercept is $\log k_F$.

In the Temkin isotherm, as the binding energy is homogeneous, the decreasing of the adsorption heat of the molecules forms in direct proportion. The Temkin model (Eq. (6)) is as follows:

$$q_e = (R.T/b)\ln K_T + (R.T/b).\ln C_e \quad (6)$$

R is gas constant 8.314 (J.mol/K), T is temperature (K), and C_e is equilibrium concentration. B_T is given in Eq. (7):

$$B_T = R.T/b \quad (7)$$

b is the Temkin isotherm constant and K_T is the equilibrium binding constant (Lg^{-1}) (Okumus and Dogan, 2019).

Dubinin and Radushkevich (D-R) isotherm is explained by the theory of potential change on the in homogeneous contact surface. Dubinin-Radushkevich (D-R) model is given in Eq. (8), and is given in Eq. (9):

$$\ln q_e = \ln q_m - K_{DR}\epsilon^2 \quad (8)$$

$$\epsilon = [1 + 1/C_e] \quad (9)$$

E is defined as the average of the adsorption energy and allows us to predict the adsorption mechanism. The equation is as given in Eq. (10):

$$E = (1/\sqrt{2K_{DR}}) \tag{10}$$

Here, R is the gas constant ($8.314 \text{ J mol}^{-1} \text{ K}^{-1}$), T is the absolute temperature (K), K_{DR} is the isotherm constant related to the adsorption energy, q_e is the theoretical adsorption capacity, q_m is maximum adsorption capacity, ϵ defines the Polanyi potential, and C_e is equilibrium concentration (Okumus and Dogan, 2019).

2.7.2 Kinetic Models

Adsorption kinetics is explained by pseudo-first-order, pseudo-second-order, intra-particle diffusion, and Elovich models. The equations of the pseudo-first-order and pseudo-second-order models are given (Bozkan, 2012).

The pseudo-first order model equation is given in Eq. (11):

$$\log(q_e - q_t) = \log(q_e) - (k_1/2.3030)t \tag{11}$$

q_e is adsorption capacity at equilibrium (mg/g), q_t is adsorption capacity at time t (mg/g), and k_1 is Pseudo-first order model constant (h^{-1}).

Theoretical q_e values are calculated from intercept, and k_1 is calculated from slope in the graph drawn between t and $\log(q_e - q_t)$ (Tumkor, 2018).

Equation (12) of the pseudo-second order model equation is given as follows:

$$t/q_t = 1/(k_2q_e^2) + t/q_e \tag{12}$$

q_e is adsorption amount at equilibrium (mg/g), q_t is adsorption amount at time t (mg/g), and k_2 is Pseudo-second order model constant (g/mg h^{-1}).

Theoretical q_e data is calculated from the slope of the graph drawn between t and t/q_t , and k_2 is calculated from intercept (Okumus and Dogan, 2019; Tumkor, 2018).

Elovich model is used to determine the adsorption and desorption kinetics of inorganic adsorbates on the surface (Erkurt, 2015). The linear equation of Elovich equation is as given in Eq. (13):

$$q_t = 1/\beta \ln(\alpha \cdot \beta) + 1/\beta \ln t \tag{13}$$

β is constant related to adsorption activation energy (g/mg), and α is initial adsorption rate in Elovich kinetic model (mg/g.min). These values can be found

by using the slope and intercept of the versus q_t versus $\ln t$ graph (Bucak, 2020).

Adsorption includes adsorbate mass exchange, surface diffusion, and pore diffusion. The linear version of the intra-particle diffusion model equation is as given in Eq. (14):

$$q_t = K_{id}t^{1/2} + C \tag{14}$$

In this equation, K_{id} indicates the intra-particle diffusion rate constant ($\text{mg/g} \cdot \text{minute}^{-1/2}$) and C indicates the boundary thickness of the layer between the adsorbent and the adsorbate. K_{id} is found from the slope of the graph drawn against q_t against $t^{1/2}$, and C is found from the intercept (Turk, 2017).

2.7.3 Thermodynamic Studies

The relationship between thermodynamic expressions is as given in Eq. (15):

$$\Delta G^\circ = \Delta H^\circ - T \cdot \Delta S^\circ \tag{15}$$

ΔG° is free energy difference (kJ/mol), ΔH° is enthalpy difference (kJ/mol), ΔS° is entropy difference (kJ/mol K),

and T is absolute temperature (K).

Equation (16) is used to find the Gibbs free energy:

$$K_c = q_e/C_e \tag{16}$$

K_c is equilibrium constant (g/L), q_e is adsorption amount of adsorbent at equilibrium (mg/g), and C_e is equilibrium concentration (mg/L). K_c is determined with the help of Eq. (17) in Eq. (18) to find the Gibbs free energy of adsorption (Sahbaz & Acikgoz, 2017):

$$\Delta G^\circ = -RT \ln K_c \tag{17}$$

R is ideal gas constant ($8.314 \text{ J}/(\text{mol} \cdot \text{K})$), T is temperature (K), and K_c is adsorption equilibrium constant.

Using Eq. (18), ΔH° is found from the slope of the line formed by plotting the $\ln K_c$ value against $1/T$ value, and ΔS° is found from the intersection point,

$$\ln K_c = (\Delta S^\circ - \Delta H^\circ/T) \times 1/R \tag{18}$$

In the study, compliance with Langmuir, Freundlich, Temkin, and Dubinin-Radushkevich isotherms were examined. Isotherm studies were

made at different humic acid concentrations (10, 55, 100 mg/L) with pH 4, temperature 25 °C, fixed 110 min time, and 0.5 g adsorbent dosage amount.

Pseudo-first order, pseudo-second-order, intra-particle diffusion model, and Elovich models were also examined. For kinetic model studies, adsorption experiments were carried out at constant solution concentration (55 mg/L), constant adsorbent dosage (0.5 g), constant pH 4, constant temperature 25 °C, and different times (15, 30, 45, 60, 75, 90, 100, 110, and 120 min).

Thermodynamic analyzes were made at three different temperatures: 25 °C, 35 °C, and 45 °C. Experimental studies were carried out with pH 4, constant 110 min time, 0.5 g adsorbent dosage amount, and 55 mg/L humic acid concentration.

3 Results and Discussion

3.1 Characterization of Adsorbents

FTR spectrum of chitosan-ECH and chitosan/ZIF 8 composite adsorbents are given in Fig. 1. As seen in Fig. 1, the peak at approximately 1570 cm^{-1} can be designated as the C=N stretching mode, while the dense and tortuous bands at 1350–1500 cm^{-1} are allied with the whole ring stretching. Bands in the 900–1350 cm^{-1} spectral region are for in-plane deflexion of the ring, while 800 cm^{-1} are known as out-of-plane deflexion. The band at 421 cm^{-1} is attributed to Zn–N stretching (Yao et al., 2013).

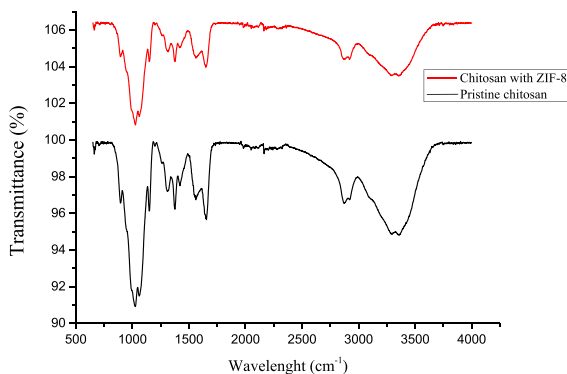


Fig. 1 Infrared spectrum of chitosan-ECH beads and chitosan/ZIF-8 composite beads

Sem images of chitosan, ZIF 8, and chitosan/ZIF 8 composite are given in the Fig. 2. For the chitosan/ZIF 8 composite, ZIF 8 crystals are interwoven with chitosan, and the SEM morphology shows that the composites consist of nano-sized particles. When the SEM photographs in the figure are examined, it is understood that ZIF 8 is compatible with chitosan.

The thermal degradation behavior of ZIF 8 added chitosan (without ECH) sphere was examined with a TGA analyzer in the temperature from 20 to 600 °C at a constant heating rate of 10 °C/min. Figure 3 shows the thermal degeneration behavior of chitosan/ZIF 8 composite spheres. TGA analysis for the beads shows only 2% weight reduction up to 100 °C. The reason for this can most likely be explained as the cancellation of water molecules from the spheres (Dehghani et al., 2018). As seen in the figure, by increasing the temperature to 400 °C and 600 °C, approximately 48% and 58% of the weight of the Chitosan/ZIF 8 composite spheres are missing, respectively. The weight reduction from 200 to 400 °C is a result of the complete degeneration of the organics of the beads. Above 400 °C, the continuous weight reduction of the spheres can be attributed to the transformation of the spheres into dissimilar oxides. The temperature at which the adsorbent begins to decompose maximum was determined as 300 °C.

XRD pattern graph was used to detect the crystal structure of the synthesized ZIF 8 and epichlorohydrin doped chitosan spheres. As seen in Fig. 4, for the XRD graph of ZIF 8-doped chitosan spheres, the intensity of the peaks increased at the 2θ angle value between 7.31 and 32.43. This increase reveals that the synthesized ZIF 8 was prepared successfully and its structure was well developed (Lin and Chang, 2015). Additionally, the XRD graph shows the highly crystalline and porous nature of ZIF 8 (Pan et al., 2011; Wong-Ng et al., 2011). In the scientific study conducted by Yao et al. (2013), XRD graphs of pure ZIF 8 synthesized using zinc nitrate hexahydrate and 2 methyl imidazole, pure chitosan, and hydrogels obtained by mixing different weights of chitosan with ZIF 8 are given. For the pure chitosan XRD graph, the intensity of the peaks increased at 2θ angle values between 15 and 25. In other graphs, as the amount of ZIF 8 in ZIF 8-doped chitosan hydrogels increases, the XRD peaks intensify between 5 and 30. In another study conducted by Dehghani et al. (2018),

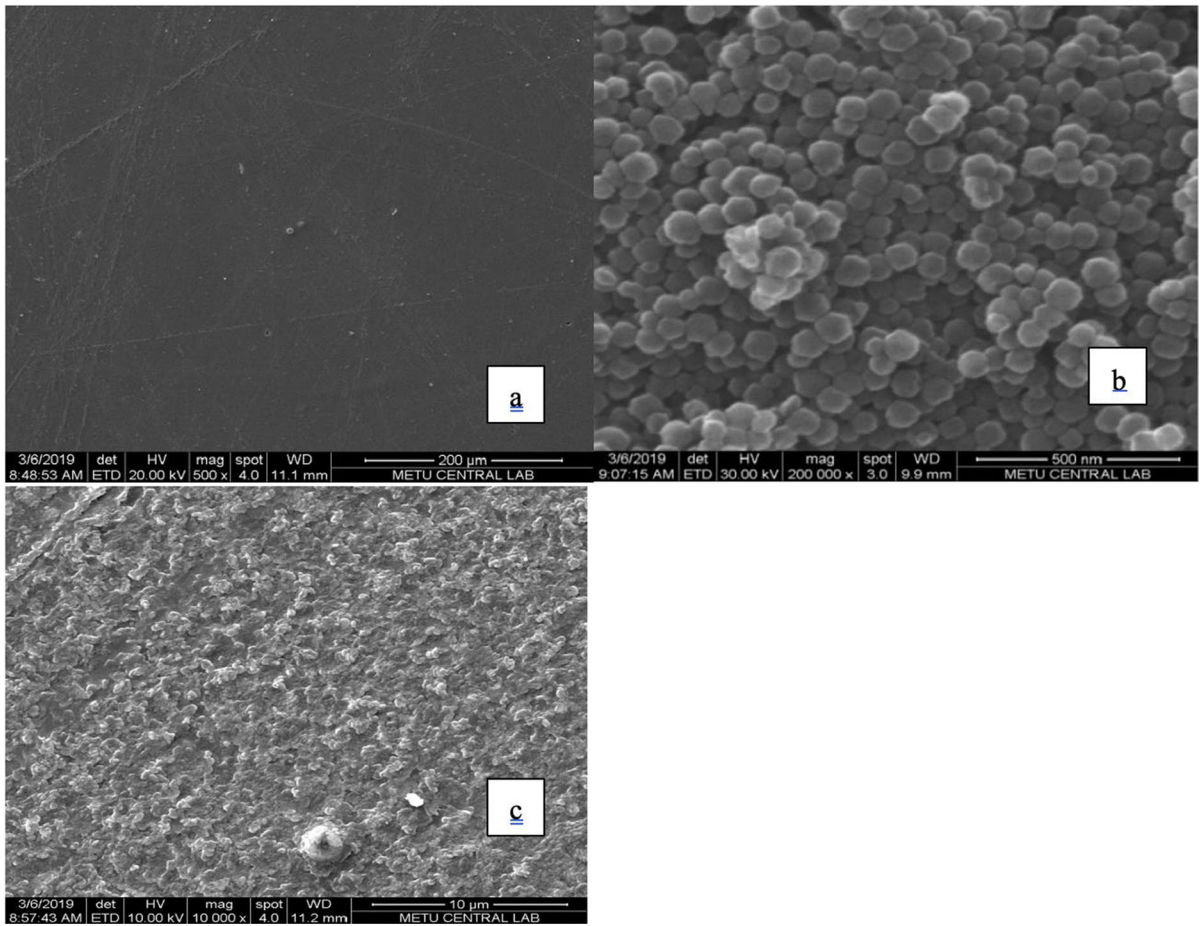


Fig. 2 Sem images of **a** chitosan beads, **b** ZIF8, and **c** Chitosan/ZIF 8 composite beads

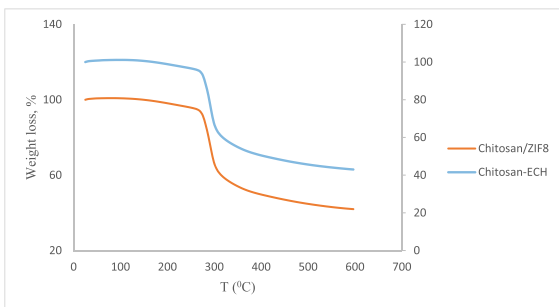


Fig. 3 TGA curve of chitosan-ECH and chitosan/ZIF 8 composite spheres

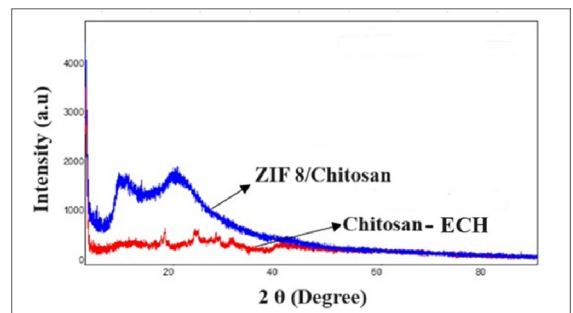


Fig. 4 XRD graphic image of ZIF 8 and ECH doped chitosan spheres

it was observed that the peaks intensified at 2θ angle values between 15 and 25 in the XRD graph for pure chitosan.

In this study, supporting the literature studies, the intensity of the peaks in the XRD graph of epichlorohydrin-doped chitosan spheres increases between 15

and 25. In addition, in the XRD graph of ZIF 8-doped chitosan spheres, the peaks intensify between 5 and 30.

3.2 Fitting Model and Optimization

Statistical data analysis with RSM was done Design Expert Student Version Programme. As seen in Table 1, chitosan adsorbent dose (0.5, 1, 1.5), humic acid solution concentration (10, 55, 100 mg/L), and temperature (25, 35, 45 °C) were used as variables, and (%) humic acid removal was entered as the response (result) into the experimental design system. In the applied Box-Behnken design model, a total of 17 experiments (5 repeated) were suggested by the system.

As a result of the optimization analysis, according to the % humic acid removal efficiency values obtained from the experiments carried out at the points of adsorbent dose (factor A), humic acid solution concentration (factor B), and temperature (factor C), the model (Eq. (19)) given in the statistical data analysis program is found as follows:

$$Y = +75,61 + 1,17A - 9,93B - 5,24C \quad (19)$$

According to this equation, factor A, that is, increasing the adsorbent dosage amount, has a positive effect on the humic acid removal efficiency. However, factors B (humic acid solution concentration) and C (Temperature) have a negative effect on the response. The increase in the numerical ratios of these factors negatively affects the humic acid removal efficiency. From the obtained model equation, it was seen that the linear model was suitable for this design.

Model compatibility results are given in Table 2 for chitosan spheres.

The fact that R^2 is close to 1 indicates the experimental data are compatible by model data. The difference between predicted R^2 and adjusted R^2 is 0.00288. Since this value is less than 0.2, it can be said that the model is compatible.

Table 2 Model compatibility result table with chitosan spheres

Model	Standard deviation	R^2	Adjusted R^2	Predicted R^2
Linear	1.77	0.9618	0.9530	0.9242
2FI	1.89	0.9662	0.9459	0.8437
Kübbik	0.5367	0.9989	0.9957	
Adequate precision: 35.4289				

In Table 3, the significance level of the effect of the variables on the response obtained as a result of the ANOVA analysis is compared with the “ F value” and “sum of squares” values. The factor with the numerically greater “ F value” and “sum of squares” values is the most effective factor on the response. Humic acid solution concentration (mg/L) has the biggest F value. Therefore, the most influential variable in the RSM is humic acid solution concentration. In other words, since F value of humic acid solution concentration (mg/L) is the biggest one, it has the most effect on removal. As the F value increases, the model accuracy increases at the same rate. In the ANOVA analysis table, the F value for model is determined as 109.04 and is seen as a significant value. As seen in the Anova analysis table, the p value was found to be less than 0.05 (Jyoti et al., 2019). It is important that the p value (probability of error value) is less than 0.05 (Hilmioğlu, 2022).

3.3 Effects of Process Variables

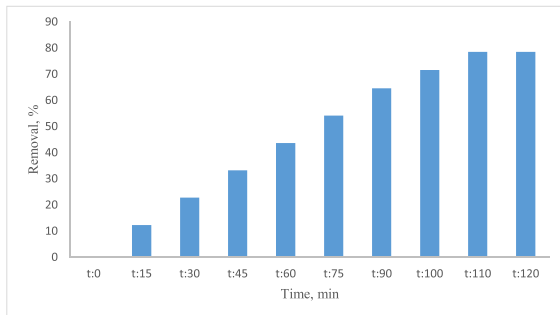
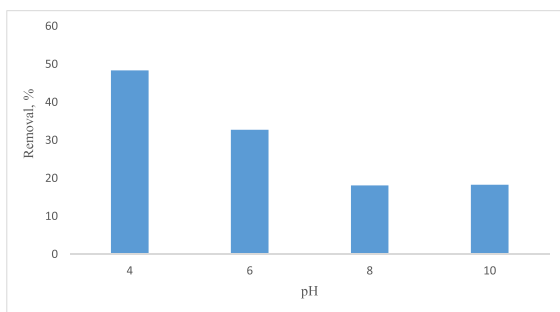
Removal efficiency change over time was examined under the conditions of pH, 4; adsorbent amount, 0.5 g; temperature, 25 °C; and concentration of humic acid, 55 mg/L. As a result of the experiments carried out with chitosan-ECH spheres, the effect of the adsorption contact time variable on the humic acid removal can be seen in Fig. 5. As seen in Fig. 5, as the adsorption time increases, the humic acid removal efficiency increases proportionally. At contact times

Table 1 Experimental factor ranges and levels with chitosan spheres

Variables	Symbols	Minimum (-1)	Mean (0)	Maximum (+1)
Adsorbent dosage (g)	A	0,5	1	1,5
Humic acid concentration (mg/L)	B	10	55	100
Temperature (°C)	C	25	35	45

Table 3 ANOVA analysis for linear model with chitosan spheres

	Sum of squares	Degrees of freedom (df)	Average of square	F value	P value
Model	1019.77	3	339.92	109.04	<0.0001
Adsorbent dosage (g)	10.97	1	3.52	0.0832	
Humic acid solution concentration (mg/L)	789.24	1	789.24	253.18	<0.0001
Temperature (°C)	219.56	1	219.56	70.43	<0.0001

**Fig. 5** Effect of different contact times with chitosan-ECH spheres on humic acid removal efficiency**Fig. 6** Effect of different pH values on humic acid removal efficiency with chitosan-ECH spheres

of 110 and 120 min, the humic acid removal was found to be 78.50% and was fixed.

The effect of solution pH value on the humic acid removal was tested for humic acid solution concentration: 55 mg/L, adsorbent dosage 0.5 g, temperature 25 °C, and contact time 110 min. As seen in Fig. 6, the pH value was set as 2, 4, 6, 8, and 10, and the humic acid removal % values were determined. As a result of the experiments, the best humic acid removal efficiency was found to be 48.34% at pH 4. Experiments were also carried out with chitosan-ECH

spheres prepared with 2% chitosan solution at pH: 4. In the experiments conducted at pH 2, the concentration values in the remaining solution increased with the contact time. Chitosan-ECH spheres did not show the function of adsorbing humic acid at this pH value, but showed the opposite effect and the hydrogel spheres dissolved in the solution.

In the study conducted by Yan et al. (2005), chitosan spheres were not studied at low pH values due to the possible dissolution of chitosan spheres in highly acidic conditions (pH < 4). Amino groups in chitosan protonated and organic complexes formed between humic acid and chitosan. For this reason, adsorption of humic acid on chitosan increases, while amino groups increases (Zhang & Bai, 2003). When the pH value in the solution was greater than 8, chitosan spheres showed a lower amount of humic acid adsorption. The reason for this situation is that an increase of the amount of hydroxide ions in the solution causes deprotonation of adsorbents (Wan Ngah et al., 2008).

Adsorption carried out with chitosan-ECH spheres for pH, 4; humic acid initial concentration, 55 mg/L; contact time, 110 min; and temperature, 25 °C; the effect of the adsorbent dosage on the humic acid removal is seen in Fig. 7. As a result of the experiments, it is seen that the humic acid removal increases as the adsorbent dosage amount increases. The increase in the removal with rising adsorbent amount is because of the increase of sorption active sites on the adsorbent surface with the increase of the adsorbent dosage (Bougdah et al., 2019). It can also be ascribed to increase in adsorption binding centers that facilitates the penetration of humic acid into the adsorption centers (Denghani et al., 2018).

Figure 8 gives a relationship between the solution concentration and removal rate for pristine chitosan-ECH and composite chitosan/ZIF 8 spheres for pH, 4; adsorbent dosage, 1.5 g; contact time, 110 min;

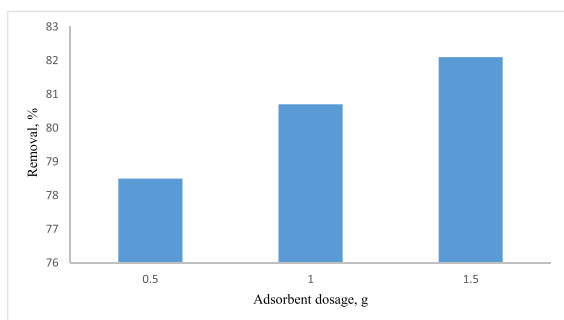


Fig. 7 Effect of different adsorbent dosage amounts on the removal efficiency with chitosan-ECH spheres

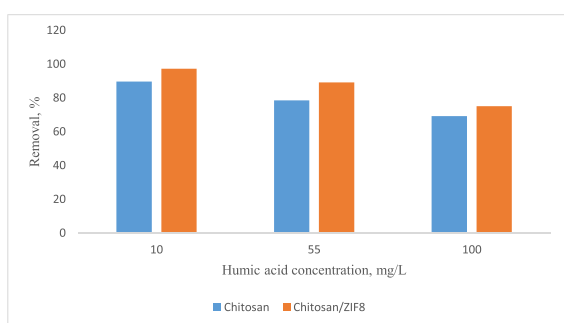


Fig. 8 Effect of different humic acid initial concentration on removal efficiency with adsorbent beads

and temperature, 25 °C. As a result of the tests with chitosan-ECH spheres obtained, the effect of the initial concentration variable of humic acid on the % humic acid removal efficiency can be seen in Fig. 8. As seen in Fig. 8, as the initial concentration of humic acid increased, the humic acid removal efficiency (%) decreased. The highest removal efficiency, with a value of 89.7%, was found when the initial concentration of humic acid was 10 mg/L. This is because when the adsorbate concentration increases, the adsorption sites (which are fixed on the adsorbent surface) decrease over time, resulting in fewer adsorption sites being available for increasing pollutant concentrations, and, as a result, the adsorption efficiency decreases (Soleimani et al., 2019). Since the amount of substance bound to the adsorption center is low when concentration is low, the amount retained by the unit adsorbent is high. As the concentration increases, adsorption decreases as the repulsive forces increase (Denghani et al., 2018).

As seen in Fig. 8, as the initial concentration of humic acid increased, the humic acid removal efficiency (%) decreased by composites also. The highest removal efficiency, with a value of 97.30%, was found when the initial concentration of humic acid was 10 mg/L by composite beads.

3.4 Comparison of Removal Efficiencies of Chitosan, ZIF 8, and Chitosan/ZIF 8 Adsorbents

Humic acid removal efficiencies from water using three different adsorbents under the same operating conditions (pH 4, adsorbent dosage 1.5 g, solution concentration 10 mg/L) are shown in Fig. 9. Humic acid removal efficiency was found to be 95.1% for chitosan-ECH spheres, 98.3% for ZIF 8, and 97.3% for chitosan/10% ZIF 8 composite, respectively. In the adsorption experiments performed using ZIF 8, the humic acid removal efficiency is higher than the other two adsorbents, but ZIF 8 is an expensive material, and it is more advantageous to use chitosan/ZIF 8 composite spheres obtained by using a smaller amount of ZIF 8 instead. In addition, ZIF 8 powder causes problems such as adhesion to the surface and filtration during use. Using composite material is easier and more advantageous than powder.

3.5 Desorption Results

The percentage yield obtained after the desorption process with epichlorohydrin and ZIF 8-doped chitosan spheres at different contact times and with 1 M HCl acid is as shown in the table. As seen in Table 4, the desorption efficiency of ZIF 8-doped chitosan spheres is higher than chitosan-ECH spheres. The

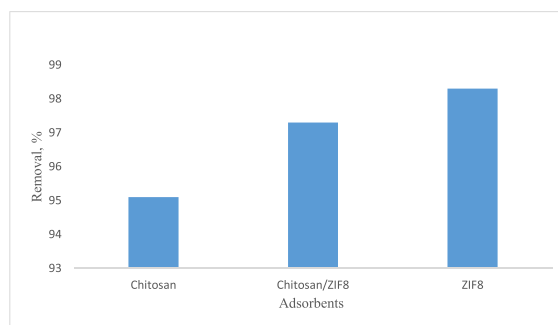


Fig. 9 Comparison of humic acid removal efficiency with different adsorbent types

Table 4 Desorption results using different adsorbents

Chitosan-ECH beads	Desorption time (min)	Desorption (%)
	60	5.8
	90	15
	120	20.9
Chitosan/ZIF 8 beads	Desorption time (min)	Desorption (%)
	60	20
	90	45.8
	120	82.5

highest desorption efficiency was found to be 82.5% for ZIF 8-doped chitosan spheres with a contact time of 120 min. Compared to chitosan-ECH spheres, the desorption efficiency increased approximately fourfold. These results are directly proportional to the desorption capacities; we obtained with the Elovich kinetic model data. In the study conducted by Wan Ngah et al. (2008), epichlorohydrin-doped chitosan spheres were contacted with 10 mg/L humic acid concentration for 1 h and filtered and dried. Desorption was carried out with the dried spheres at 1×10^{-6} M HCl concentrations using different contact times (30, 120, 180 min). The best desorption efficiency was found to be 61.2% with 1 M HCl and 180 min contact time (Wan Ngah et al., 2008). It has been observed that cross-linked chitosans swell without dissolving in organic acids. Therefore, despite

using high concentrations of HCl, humic acid could not be completely removed (Wan Ngah et al., 2008).

3.6 Isotherm Models

Compliance with Langmuir, Freundlich, Temkin, and Dubinin-Radushkevich isotherms on the removal of humic acid from water with chitosan-ECH spheres was examined. Isotherm studies were performed at different humic acid concentrations (10, 55, 100 mg/L) with pH, 4; T, 25 °C; 110 min time; and 0.5 g adsorbent dosage.

Data obtained from all isotherm models are given in Table 5. It was observed that the R^2 values of the Temkin and Dubinin-Radushkevich isotherms were smaller than the Langmuir and Freundlich isotherms. Therefore, it was decided that the current process does not comply with these isotherms.

As given in Table 6, experimental and theoretical q_e values for the Freundlich isotherm are very close to each other. Therefore, the current adsorption appears to obey the Freundlich isotherm. In addition, K_L values were found to be 0.44, 0.127, and 0.074, depending on different humic acid concentration values. An exponential n value greater than 1 is an indicator of a suitable adsorption process. According to the Freundlich isotherm model, the multilayer adsorption process occurs on the heterogeneous adsorbent surface because of the various of adsorptive sites (Okumus

Table 5 Isotherm parameters for humic acid adsorption from water with chitosan-ECH spheres

Isotherm model	Parameter	Value
Langmuir	q_m (mg g ⁻¹)	15.64
	R^2	0.999
	K_L (L mg ⁻¹)	0.44 (10 mg/L)
		0.127 (55 mg/L)
	0.074 (100 mg/L)	
Freundlich	R^2	0.997
	n (g L ⁻¹)	1.63
	K_F ((mg g ⁻¹) (L mg ⁻¹)) ^{1/n}	1.79
Temkin	B_T	726.04
	K_T (L mg ⁻¹)	1.49
	R^2	0.9724
	Dubinin-Radushkevich	q_m (mg g ⁻¹)
K_{DR} (mol ² j ⁻²)		0.65
E (kJ mol ⁻¹)		37
R^2		0.9557

Table 6 Experimental and theoretical q_e values for Langmuir and Freundlich isotherms for chitosan-ECH spheres

Isotherm	Experimental q_e (mg/g)	Theoretical q_e (mg/g)
Langmuir isotherm	8.64	9.36
Freundlich isotherm	8.64	8.13

and Dogan, 2019; Wan Ngah, 2008; Sahbaz & Acikgoz, 2017).

Adsorption experiments were carried out with chitosan spheres with 10% ZIF8 additive (without ECH) under optimum working conditions obtained from the adsorption experimental studies conducted for chitosan with the statistical data analysis program. Compliance with Langmuir, Freundlich, Temkin, and D-R isotherms was examined on the removal of humic acid from water using spheres prepared with 10% ZIF 8 added and chitosan (without ECH) solution. Isotherm studies were carried out at different humic acid concentrations (10, 55, 100 mg/L) with pH 4, T 25 °C, 100 min time, and 1.5 g adsorbent dosage.

In order to determine the isotherm model in which the adsorption process of humic acid from water and ZIF 8-doped chitosan spheres is compatible, the R^2 values of the graphs were examined (Table 7). When examined, the R^2 value of the Langmuir isotherm was found to be higher. Therefore, it appears that the current adsorption is compatible with the Langmuir

isotherm (Okumus and Dogan, 2019). In addition, the K_L values, which are dimensionless numbers belonging to the Langmuir isotherm, were found to be 0.14, 0.029, 0.251, and 0.016.

3.7 Kinetic Models

In the study conducted with 2% chitosan-ECH spheres, four different kinetic models were used: pseudo-first order, pseudo-second order, intra-particle diffusion model, and Elovich.

The results in the figures give lines with high R^2 values. In addition, experimental q_e values are compatible with the calculated q_e values, as seen in Table 8. Therefore, the pseudo-first-order kinetic model is suitable for this process.

The model with the highest R^2 value is the intra-particle diffusion model. The data appear to fit this model. However, since q_e cannot be calculated theoretically in this model, no comment can be made about whether q_e is close to the experimental one. Since q_e theoretical and q_e experimental values can be calculated with the pseudo-first-order kinetic model and the pseudo-second-order kinetic model, when approached from this perspective and the R^2 value is above 0.9, it can be said that the data is compatible with the pseudo-first-order kinetic model.

Adsorption experiments were carried out with chitosan spheres with 10% ZIF8 additive (without ECH) under optimum working conditions obtained with the

Table 7 Isotherm parameters for humic acid adsorption from water with chitosan/ZIF 8 spheres

Isotherm model	Parameter	Value
Langmuir	q_m (mg g ⁻¹)	4.64
	R^2	0.9983
	K_L	0.14 (10 mg/L)
		0.029 (55 mg/L)
Freundlich	R^2	0.987
	n (g L ⁻¹)	2.16
	K_F ((mg g ⁻¹)(L mg ⁻¹)) 1/n	1.24
Temkin	B_T	2612
	K_T (L mg ⁻¹)	1.00
	R^2	0.9915
Dubinin-Radushkevich	q_m (mg g ⁻¹)	4.07
	K_{DR} (mol ² j ⁻²)	0.1252
	E (kJ mol ⁻¹)	20
	R^2	0.9628

Table 8 Calculated data of kinetic models for chitosan-ECH spheres

Kinetic model	Constants	q_e (mg g ⁻¹) (calculated)	q_e (mg g ⁻¹) (experimental)	R^2
Pseudo-first-order	K_1 (dk ⁻¹): 0,0214	11.76	8.64	0.9295
Pseudo-second-order	K_2 (mg g ⁻¹ .min ⁻¹): 0,000034	51.02	8.64	0.818
Elovich kinetic	Desorption constant β : 0.32 mg/g Adsorption velocity constant α : 16,56 (g.g ⁻¹ .min ⁻¹)	-	-	0.877
Intraparticle diffusion	Intraparticle diffusion velocity constant K_{id} : 1.0934 (mg.g ⁻¹ .min. ^{1/2})	-	-	0.9864

Table 9 Kinetic parameters for chitosan/ZIF8 composite

Kinetic model	Constants	q_e (mg g ⁻¹) (calculated)	q_e (mg g ⁻¹) (experimental)	R^2
Pseudo-first-order	K_1 : 0.002303 (min ⁻¹)	0.188	0.65	0.0022
Pseudo-second-order	K_2 : 0.016 (mg g ⁻¹ .min ⁻¹)	1.03	0.65	0.9676
Elovich kinetic	β : 4.91 mg/g α : 1.32 (g.g ⁻¹ .min ⁻¹)	-	-	0.9455
Intraparticle diffusion	K_{id} : 0.0708 (mg.g ¹ .min. ^{1/2})	-	-	0.9439

statistical data analysis program from the adsorption experimental studies carried out with spheres prepared with chitosan-ECH. Experimental conditions for kinetic model studies are as follows: pH 4, adsorbent dosage 1.5 g, solution concentration 10 mg/L, temperature 25 °C, and different times (15, 30, 45, 60, 75, 90, 100, 110 min).

As a result of the kinetic studies in the Table 9, it was seen that pseudo-second-order model was the most suitable model. The reason for this is that it has a higher regression coefficient compared to other models.

3.8 Thermodynamics Studies

Thermodynamic analyzes were performed at three different temperatures: 25 °C, 35 °C, and 45 °C. Experimental studies were carried out with pH 4, 110 min time, 0.5 g adsorbent dosage, and 55 mg/L humic acid concentration. The results are given in Table 10.

When Table 10 was examined, the fact that $\Delta H^0 < 0$ shows that this process is not endothermic

Table 10 Thermodynamic study for chitosan-ECH spheres

Temperature T (K)	ΔH^0 (kJ mol ⁻¹)	ΔS^0 (kJ mol ⁻¹ K ⁻¹)	ΔG^0 (kJ mol ⁻¹)
298	-25.62	-0.088	0.77
308	-25.62	-0.088	1.72
318	-25.62	-0.088	2.55

(Okumus and Dogan, 2019) and that low temperatures are to the advantage of adsorption. In the experimental study conducted by Aslan et al., as the temperature of the solution increases, the amount of Gibbs free energy decreases, providing better adsorption at high temperatures, but in our study, a directly proportional increase in Gibbs energy is observed with the increase in temperature of the solution (Aslan et al., 2021).

This once again confirmed the result that we proved in the statistical analysis program that high temperature negatively affects humic acid adsorption (Aslan et al., 2021). A negative value of ΔS^0 indicates a decrease in the amount of adsorbed

substance at the solute and solution interface (Orbak, 2009).

4 Conclusions

Isotherm, kinetic, and thermodynamic studies were carried out with chitosan-ECH spheres, and the fact that the most appropriate model with the calculated data was Freundlich, $n < 1.63$, and the E value in the D-R isotherm model was 37 kJ/mol proved that the process was chemical. In thermodynamic studies carried out at temperatures of 25, 35, and 45 °C, the negative ΔH° enthalpy value confirms that the adsorption process is an exothermic study, that is, it releases heat to the outside. It also shows that working at low temperature values increases the adsorption efficiency. As a result of experimental adsorption studies, the effects of contact time, solution pH value, humic acid initial concentration, and adsorbent dosage change on humic acid removal efficiency (%) were examined. In order to determine the optimum experimental working conditions, adsorption tests were carried out with a total of 17 experiments, optimized with RSM. The optimum experimental conditions were determined as 1.5 g adsorbent dosage amount, 10 mg/L humic acid initial concentration, and 25 °C temperature. For spheres produced with chitosan/ZIF 8 composite, ZIF 8 suspension ratio was tried as 10%, 20%, and 30%, but the best humic acid removal efficiency was obtained by adding 10% ZIF 8 suspension. Adsorption experiments were carried out with chitosan, ZIF 8, and chitosan/ZIF8 adsorbents under the determined optimum parameters, and the humic acid removal efficiency was found to be 95.1%, 98.3%, and 97.3%, respectively. The highest humic acid removal efficiency was obtained in adsorption experiments performed with ZIF 8 powder. However, since ZIF 8 powder is difficult to separate from the solution and is an expensive material, it is more advantageous to use it by creating composite spheres with biobased chitosan. Likewise, isotherm and kinetic studies were conducted with sphere adsorbents obtained with chitosan/ZIF 8 composite, and it was determined that the most suitable models were Langmuir and pseudo-second-order kinetic models. At the same time, it was concluded that there was a chemical adsorption with the E value in the D-R isotherm model being 20 kJ/mol. Desorption processes were carried out with 1 M HCl acid using chitosan-ECH sphere and

chitosan/ZIF 8 sphere adsorbents with contact times of 60, 90, and 120 min, and it was observed that desorption efficiencies increased with increasing contact time. The desorption efficiency was found to be 20.9% and 82.5%, respectively. When maximum adsorption capacity q_m values were compared, it was seen that pure chitosan spheres had higher adsorption capacity per unit adsorbent than composite spheres.

Funding Open access funding provided by the Scientific and Technological Research Council of Türkiye (TÜBİTAK). This study was supported by the scientific research projects unit (BAP) of Kocaeli University by Project No FMP-2022-2779.

Data Availability The datasets used and/or analyzed during the current study are available from the corresponding author upon reasonable request.

Declarations

Ethics Approval Not applicable.

Conflict of Interest The authors declare no competing interests.

Open Access This article is licensed under a Creative Commons Attribution 4.0 International License, which permits use, sharing, adaptation, distribution and reproduction in any medium or format, as long as you give appropriate credit to the original author(s) and the source, provide a link to the Creative Commons licence, and indicate if changes were made. The images or other third party material in this article are included in the article's Creative Commons licence, unless indicated otherwise in a credit line to the material. If material is not included in the article's Creative Commons licence and your intended use is not permitted by statutory regulation or exceeds the permitted use, you will need to obtain permission directly from the copyright holder. To view a copy of this licence, visit <http://creativecommons.org/licenses/by/4.0/>.

References

- Aslan, S., Yıldız, S., & Öztürk, M. (2021). Biosorption of Cu²⁺ from synthetic wastewater by tea waste sorbent: Kinetics, equilibrium and thermodynamics. *Pamukkale University Journal of Engineering Sciences*, 27(3), 359–367. <https://doi.org/10.5505/Pajes.2020.273>
- Bougdah, N., Bousba, S., Messikh, N., & Magri, P. (2019). Adsorption of humic acid onto chitosan: Isothermal and kinetic studies. *Asian Jr of Microbiol Biotech Env Science Global Science Publications*, 21(4), 896–900.
- Bozkan, H. (2012). *The removal of azo dyes by using olive waste (pomace) and adsorption method*. Master's Thesis, Selcuk University, Institute of Science and Technology, Environmental Engineering Department. 327037, 17–18.

- Bucak, S. (2020). *Investigation of the removal of Br13 dye from aqueous solutions with the use of sodium dodecyl sulphate modified montmorillonite clay*. Master's Thesis, Van Yuzuncu Yil University, Institute of Science and Technology, Environmental Engineering Department. 608395, 25–27.
- Dehghani, M. H., Ghadermazi, M., Bhatnagar, A., Sadighara, P., Jahed-Khaniki, G., Heibati, B., & McKay, G. (2016). Adsorptive removal of endocrine disrupting bisphenol A from aqueous solution using chitosan. *Journal of Environmental Chemical Engineering*, 4(3), 2647–2655. <https://doi.org/10.1016/j.jece.2016.05.011>
- Dehghani, M. H., Dehghan, A., & Najafpoor, A. (2017). Removing reactive red 120 and 196 using chitosan/zeolite composite from aqueous solutions: Kinetics, isotherms, and process optimization. *Journal of Industrial and Engineering Chemistry*, 51, 185–195. <https://doi.org/10.1016/J.JIEC.2017.03.001>
- Dehghani, H. M., Zarei, A., Mesdaghinia, A., Nabizadeh, R., Alimohammadi, M., Afsharnia, M., & McKay, G. (2018). Production and application of a treated bentonite–chitosan composite for the efficient removal of humic acid from aqueous solution. *Chemical Engineering Research and Design*, 140, 102–115. <https://doi.org/10.1016/j.cherd.2018.10.011>
- Erkurt, F. E., & Balci, B. (2015). Investigation of adsorption of reactive black 5 dye onto activated carbon by using kinetic and adsorption models. *Cukurova University Journal of the Faculty of Engineering and Architecture*, 30(1), 257–269. <https://doi.org/10.21605/cukurovaummf.242787>
- Gundag O. (2017). *Comparison of humic acid removal alternatives in water*. Master's Thesis, Namik Kemal University, Institute of Science and Technology. 80.
- Hartono, T., Wang, S., Ma, Q., & Zhu, Z. H. (2009). Layer structured graphite oxide as a novel adsorbent for humic acid removal from aqueous solution. *Journal of Colloid and Interface Science*, 333(1), 114–119. <https://doi.org/10.1016/J.Jcis.2009.02.005>
- Hilmioglu, N. (2022). Optimization of synthesis of ethyl acetate by response surface method and investigation of reactive sorption effect of hydrogel in synthesis. *Avrupa Bilim ve Teknoloji Dergisi*, 35, 94–101. <https://doi.org/10.31590/ejosat.1061611>
- Jampa, K., S., Unnarkat, A.P., Vanshpati, R., Pandian, S., Sinha, M.K., & Dharaskar, S. (2020). Adsorption and recyclability aspects of humic acid using nano-ZIF-8 adsorbent. *Environmental Technology & Innovation*, 19. <https://doi.org/10.1016/J.Eti.2020.100927>
- Jyoti, G., Keshav, A &, Anandkumar, J. (2019). Optimization of Esterification of Acrylic Acid and Ethanol by Box-Behnken Design of Response Surface Methodology. *Indian Journal of Chemical Technology*, 26, 89–94. (Online)
- Khan, S., Kim, J., Sotto, A., & Van Der Bruggen, B. (2015). Humic acid fouling in a submerged photocatalytic membrane reactor with binary TiO₂–ZrO₂ particles. *Journal of Industrial and Engineering Chemistry*, 21, 779–786. <https://doi.org/10.1016/j.jiec.2014.04.012>
- Lin, A. K. Y., & Chang, H. A. (2015). Efficient adsorptive removal of humic acid from water using zeolitic imidazole framework-8 (ZIF-8). *Water, Air, and Soil Pollution*, 226(10), 2–17. <https://doi.org/10.1007/S11270-014-2280-7>
- Lin, J., & Zhan, Y. (2012). Adsorption of humic acid from aqueous solution onto unmodified and surfactant-modified chitosan/zeolite composites. *Chemical Engineering Journal*, 200, 202–213. <https://doi.org/10.1016/J.Cej.2012.06.039>
- Lorenc-Grabowska, E., & Gryglewicz, G. (2005). Adsorption of lignite-derived humic acids on coal-based mesoporous activated carbons. *Journal of Colloid and Interface Science*, 284(2), 416–423. <https://doi.org/10.1016/j.jcis.2004.10.031>
- Mathur, N. K., & Narang, C. K. (1990). Chitin and chitosan, versatile polysaccharide from marine animals. *Journal of Water Resource and Protection*, 67(11), 938. <https://doi.org/10.1021/Ed067p938>
- Mohammed, M.A., & Shitu, A. (2014). Removal of methylene blue using low cost adsorbent: a review. *Research Journal of Chemical Sciences*, 4 (1), 91–102. E-ISSN : 2231 - 606X.
- Oktor, K., & Hilmioglu, N. (2021). Removal of ammonium from aqueous solutions by adsorption processes using environment friendly natural biopolymer chitosan. *Fresenius Environmental Bulletin*, 30(2A), 1970–1976.
- Oktor, K., Yuzer, N. Y., Hasirci, G., & Hilmioglu, N. (2023). Optimization of removal of phosphate from water by adsorption using biopolymer chitosan beads. *Water, Air and Soil Pollution : An International Journal of Environmental Pollution*, 234(4), 1–14. <https://doi.org/10.1007/s11270-023-06230-x>
- Okumus, Z. C. & Dogan T. H. (2019). Removal of water from biodiesel with resin: Isothermal, kinetic and thermodynamic investigation of adsorption. *European Journal of Science and Technology*, 15, 561–570. <https://doi.org/10.31590/Ejosat.535977>.
- Orbak I (2009). *Removal of environmental pollutants by using activated carbon*. Doctoral thesis, Istanbul Technical University, Institute of Science and Technology. 56.
- Pan, Y., Heryadi, D., Zhou, F., Zhao, L., Lestari, G., Su, H., & Lai, Z. (2011). Tuning the crystal morphology and size of zeolitic imidazolate framework-8 in aqueous solution by surfactants. *Cryst. Eng. Comm*, 13(23), 6937–6940. <https://doi.org/10.1039/C1CE05780D>
- Park, S., Ni, Z., Côté, P., Choi, Y., & Huang, R. (2006). Exceptional chemical and thermal stability of zeolitic imidazolate frameworks. *Proceedings of the National Academy of Sciences*, 103(27), 10186–10191. <https://doi.org/10.1073/Pnas.0602439103>
- Park, J., Jiang, Q., Feng, D., Mao, L., & Zhou, H. C. (2016). Size-controlled synthesis of porphyrinic metal-organic framework and functionalization for targeted photodynamic therapy. *Journal of the American Chemical Society*, 138(10), 3518–3525. <https://doi.org/10.1021/jacs.6b00007>
- Rodrigues, D. S. C., Madeira, M., & L. & Boaventura, A. R. R. (2009). Optimization of the azo dye Procion Red H-EXL degradation by Fenton's reagent using experimental design. *Journal of Hazardous Materials*, 164(2–3), 987–994. <https://doi.org/10.1016/j.jhazmat.2008.08.109>
- Sahbaz, D. A., & Acikgoz, C. (2017). Cross-linked chitosan/marble powder composites for the adsorption of dimazol blue. *Water Science & Technology*, 76 (10), <https://doi.org/10.2166/Wst.2017.447>.
- Soleimani, H., Mahvi, A., Yaghmaeian, K., Abbasnia, A., Sharafi, K., Alimohammadi, M., & Zamanzadeh, M. (2019). Effect of modification by five different acids

- on pumice stone as natural and low-cost adsorbent for removal of humic acid from aqueous solutions-application of response surface methodology. *Journal of Molecular Liquids*, 290, 111–118. <https://doi.org/10.1016/J.Molliq.2019.111181>
- Soylu S. (2011). *Physical characterization of natural organic matter in drinking water*. Master's Thesis, Pamukkale University, Institute of Science and Technology, 26.
- Tumkor, E. (2018). *Investigation of adsorption of oleic acid from sunflower oil by using Amberlyst 21 as an adsorbent*. Master's Thesis, Kocaeli University, Institute of Science and Technology, 522397.
- Turk, O. (2017). *Adsorption of azure a on raw and modified vermiculite*. Master's Thesis, Bingol University, Institute of Science and Technology, 492649.
- Venna, S. R., Jasinski, J. B., & Carreon, M. A. (2010). Structural evolution of zeolitic imidazolate framework-8. *Journal of the American Chemical Society*, 132(51), 18030–18033. <https://doi.org/10.1021/ja109268m>
- Wan Ngah, W. S., Hanafiah, M. A. K. M., & Yong, S. S. (2008). Adsorption of humic acid from aqueous solutions on crosslinked chitosan–epichlorohydrin beads: Kinetics and isotherm studies. *Colloids and Surfaces B: Biointerfaces*, 65(1), 18–24. <https://doi.org/10.1016/j.colsurfb.2008.02.007>
- Wan Ngah, W. S., & Musa, A. (1998). Adsorption of humic acid onto chitin and chitosan. *Journal of Applied Polymer Science*, 69, 2305–2310. [https://doi.org/10.1002/\(SICI\)1097-4628\(19980919\)69:12<2305::AID-APP1>3.0.CO;2-C](https://doi.org/10.1002/(SICI)1097-4628(19980919)69:12<2305::AID-APP1>3.0.CO;2-C)
- Wang, M., Liao, L., Zhang, X., & Li, Z. (2012). Adsorption of low concentration humic acid from water by palygorskite. *Applied Clay Science*, 67, 164–168. <https://doi.org/10.1016/j.clay.2011.09.012>
- Wong-Ng, W., Kaduk, J. A., Espinal, L., Suchomel, M. R., Allen, A. J., & Wu, H. (2011). High-resolution synchrotron X-ray powder diffraction study of bis(2-methylimidazolyl)-zinc, C8H10N4Zn (ZIF-8). *Powder Diffraction*, 26(3), 234–237. <https://doi.org/10.1154/1.3625701>
- Yan, W. L., & Bai, R. (2005). Adsorption of lead and humic acid on chitosan hydrogel beads. *Water Research*, 39(4), 688–698. <https://doi.org/10.1016/j.watres.2004.11.007>
- Yao, J., Chen, R., Wang, K., & Wang, H. (2013). Direct synthesis of zeolitic imidazolate framework-8/chitosan composites in chitosan hydrogels. *Microporous and Mesoporous Materials*, 165, 200–204. <https://doi.org/10.1016/j.micromeso.2012.08.018>
- Zhang, X., & Bai, R. (2003). Mechanisms and kinetics of humic acid adsorption onto chitosan-coated granules. *Journal of Colloid and Interface Science*, 264(1), 30–38. [https://doi.org/10.1016/S0021-9797\(03\)00393-X](https://doi.org/10.1016/S0021-9797(03)00393-X)

Publisher's Note Springer Nature remains neutral with regard to jurisdictional claims in published maps and institutional affiliations.